9. Kokotovic, P. V., J. B. Cruz, et al., *IEEE Proc.*, **56**, 1318 (1968).
10. Kriendler, F., *Grumman Aircraft Tech. Rept.*, AFFDL-TR-66-209 (Apr. 1967).
11. ———, *Intern. J. Control*, **2**, 171 (1967).
12. ———, *J. Franklin Inst.*, **285**, 26 (1968).
13. ———, *IEEE Trans. Auto. Control*, **13**, 254 (1968).
14. ———, *Intern. J. Control*, **8**, 89 (1968).
15. Lapidus, L., and R. Luus, "Optimal Control of Engineering Processes, Blaisdell, Waltham, Mass. (1967).
16. Lee, E. S., *Ind. Eng. Chem. Fundamentals*, **3**, 373 (1964).
17. McClamroch, N. H., and J. K. Aggarwal, *Proc. 5th Allerton Conf.* (Oct. 1967).
18. ———, *J. Franklin Inst.*, **285**, 483 (1968).
19. Pagurek, B., *Intern. J. Control*, **1**, 33 (1965).
20. ———, *IEEE Trans. Auto. Control*, **10**, 178 (1965).
21. Pontryagin, L. S., et al., "The Mathematical Theory of Optimal Processes," Interscience, New York (1962).
22. Rissanen, J. J., and R. Durbeck, *J. Basic Eng.*, **89**, 311 (1967).
23. ———, *IEEE Trans. Auto. Control*, **11**, 530 (1966).
24. Rohrer, R. A., and M. Sobral, *ibid.*, **10**, 43 (1965).
25. Sage, A. P., "Optimum Systems Control," Prentice-Hall, Englewood Cliffs, N.J. (1968).
26. Seinfeld, J. H., *AIChE J.*, **15**, 57 (1969).
27. ———, *Can. J. Chem. Eng.*, **47**, 212 (1969).
28. Sobral, M., *IEEE Proc.*, **56**, 1644 (1968).
29. Tomovic, R., "Sensitivity Analysis of Dynamic Systems," McGraw-Hill, New York (1963).
30. Weinrich, S. D., Ph.D. dissertation, Princeton Univ., (Sept. 1970).
31. Werner, R. A., and J. E. Cruz, *IEEE Trans. Auto. Control*, **13**, 621 (1968).
32. Witsenhausen, H. S., *ibid.*, **10**, 495 (1965).
33. *Ibid.*, **11**, 620 (1966).

Manuscript received November 24, 1970; revision received March 18, 1971; paper accepted March 19, 1971.

Entrance Region Flow of Polymer Melts

CHANG DAE HAN

Department of Chemical Engineering

Polytechnic Institute of Brooklyn, Brooklyn, New York 11201

An experimental study has been made to investigate polymer melt flow in the entrance region of a circular tube. For the study, a capillary rheometer was used to measure wall normal stresses in polymer melts in the reservoir and along the axis of the capillary. In order to investigate the influence of reservoir diameter on the entrance pressure drops, reservoir-to-capillary diameter (D_R/D) ratios of 3, 6, 9, and 12 were used, with the capillary length-to-diameter (L/D) ratio being 20 and the capillary diameter being 0.125 in. Analysis of the experimental data shows that the entrance pressure drop increases and then levels off as D_R/D ratio is increased. A correlation between the dimensionless entrance pressure drop and Reynolds number has been obtained, which follows the creeping flow analysis by Weissberg over the range of the area contraction ratio studied, $0.00694 \leq \beta \leq 0.111$.

When fluid enters a tube from a large reservoir, the velocity profile starts to develop and continues to change until a certain distance is reached beyond which flow is said to be fully developed. The finite length of tube required for attaining a fully developed flow profile is known as the entrance length. Clearly, the magnitude of the entrance length is dependent upon the viscosity of the fluid, the diameters of the tube and the reservoir, velocity of the fluid (for Newtonian fluids), and the elastic properties (for viscoelastic fluids). The criterion for determining fully developed flow in viscoelastic fluids (for example, polymer melts) has been a controversial subject. A conventional criterion, such as the constant pressure gradient in the tube, does not seem sufficient, although necessary, for viscoelastic fluids, while of course the same criterion has been well accepted for Newtonian fluids. Conditions other than the constant pressure gradient in polymer melt flow have recently been suggested by Han and Charles (*1*).

As one may surmise, the entrance length problem is intimately related to the flow situation in the reservoir. It is a well-established fact that viscoelastic fluids start to build their streamline in the reservoir before they actually reach the entrance of the tube. It has also been known for a long time that when viscoelastic fluids, in particular polymer melts, flow from a reservoir into a circular tube, they undergo excessively large pressure drops. This pressure drop is considerably greater for polymer melts than for Newtonian fluids. There is ample evidence that the viscosity of the material alone cannot explain such excessive pressure drops. And some efforts (*2* to *4*) have been made to explain the excessive pressure drops of polymer melts in terms of the elastic properties of the material.

In the past, attempts have been made by several investigators (*5* to *8*) to relate the entrance pressure drops (or the entrance lengths) theoretically both to the rheological properties of non-Newtonian fluids and to the geometries of the reservoir and tube as well. Invariably these investigators approached the problem by means of boundary-layer analysis. However, applicability of their analyses to polymer melt flow in the entrance region is highly questionable, because in most flow situations of practical interest, polymer melts yield exceedingly low Reynolds num-

bers due to the high values of their viscosities. Hence a creeping flow approach seems to be more appropriate to solve analytically the entrance region problem than the boundary-layer analysis. Weissberg (9) used creeping flow analysis for Newtonian fluid, but so far no successful analysis has been reported in the literature dealing with viscoelastic fluids in the entrance region.

In view of the complexity of flow conditions in the entrance region, an experimental approach would seem to be quite helpful, at least for the time being, to obtain some useful correlation between the entrance pressure drops and rheological properties of polymer melts and geometries of the reservoir and tube as well. Unfortunately, little has been published in the literature of experimental data of polymer melt flow in the entrance region, to any extent that will be useful at least for engineering design purposes. However, in recent years problems associated with polymer melt flow have become increasingly important in chemical engineering practice.

It is the purpose of this paper to present some new experimental data of the entrance pressure drops of polymer melts flowing through a circular tube. The present study investigated, in particular, the dependence of the entrance pressure drops on the reservoir-to-capillary diameter ratio.

EXPERIMENTAL

The apparatus used in the present study has been described in earlier papers (*10, 11*). In the present study, four dies were newly constructed, with reservoir diameters of 0.375, 0.750, 1.125, and 1.500 in., and each with an L/D ratio of 20, the capillary diameter being 0.125 in.

The materials used for the study were high density polyethylene (DMDJ 4309), polypropylene (Resin E115), low density polyethylene (PEP 211), and polystyrene (Styron® 686) at temperatures of 180°, 200°, 220°, and 240°C.

For the experiment, melt pressure transducers were used to measure wall normal stresses in the reservoir section and along the axis of the capillary. The axial pressure profiles were then used to obtain the entrance pressure drops. Detailed experimental procedures and the method of analyzing experimental data have been described in previous papers (*10, 11*).

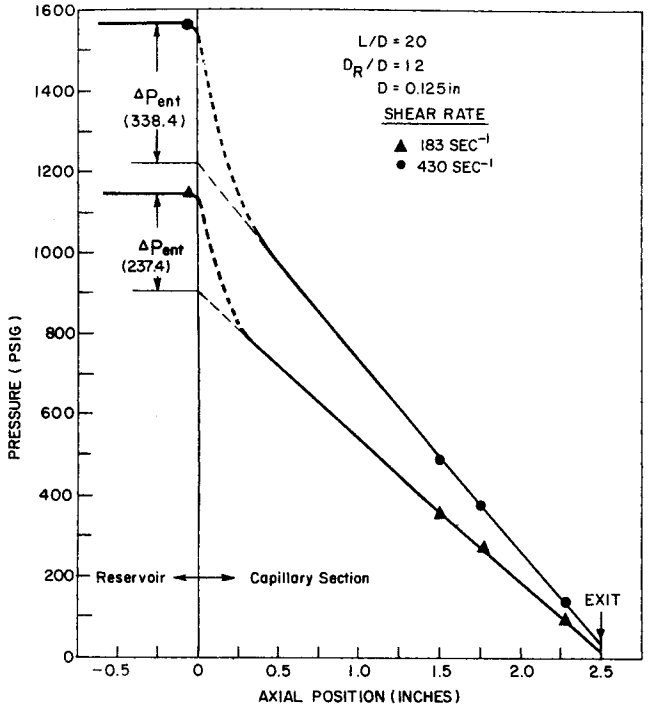

Fig. 1. Representative pressure profiles for high density polyethylene melts (L/D = 20, T = 180°C).

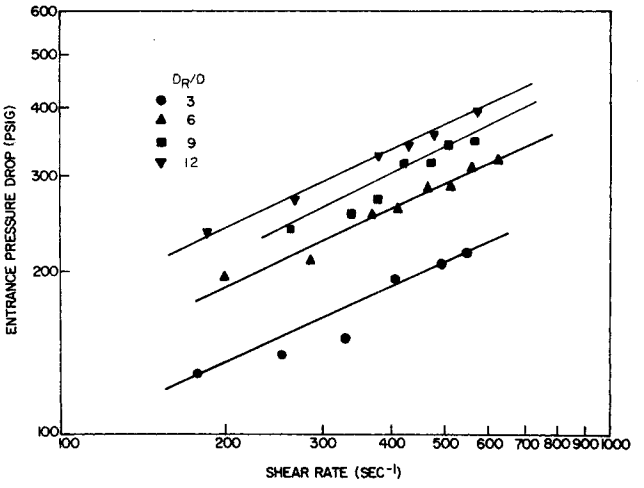

Fig. 2. Entrance pressure drop versus shear rate for high density polyethylene at 180°C.

RESULTS AND DISCUSSION

In Figure 1 are shown some representative axial pressure profiles for high density polyethylene melts at 180°C., with a D_R/D ratio of 12 and an L/D ratio of 20 (capillary diameter D is 0.125 in.). It is seen from Figure 1 that the entrance pressure drop ΔP_{ent} is clearly a function of shear rate. Similar results were obtained for D_R/D ratios of 3, 6, and 9.

It is to be noted in Figure 1 that when the straight line portions of the axial pressure profiles are extrapolated to the tube exit, considerable exit pressure (that is, nonzero gauge pressure at the tube exit) is obtained. Recent papers by Han et al. (*10, 11*) give the rheological implications of the exit pressure in the steady flow of polymer melts through circular tubes. Note also that the same authors (*11*) have performed experimental studies to test pressure-hole errors in the measurement of wall normal stresses, and found no pressure-hole errors insofar as polymer melts are concerned.

Figure 2 shows plots of the entrance pressure drops versus shear rate, with D_R/D ratio as a parameter. It is seen that a power law relation holds between the entrance pressure drop and shear rate:

$$\Delta P_{ent} = c\,\dot{\gamma}^{\,d} \qquad (1)$$

It may be interesting to note from Figure 2 that d in Equation (1) is constant, while the constant c depends on the D_R/D ratio. It may be seen further from Figure 2 that the entrance pressure drops first increase with D_R/D ratio and then level off at a D_R/D ratio of about 12. This observation is of particular interest in the design of various processing devices, such as spinnerettes and dies for film extrusion.

If the ideas set forth in the early part of this paper are valid, one should find a correlation between the dimensionless entrance pressure drops and Reynolds number. Such a correlation is also very important for design purposes. Recently Sylvester and Rosen (*12*) proposed the following relationship

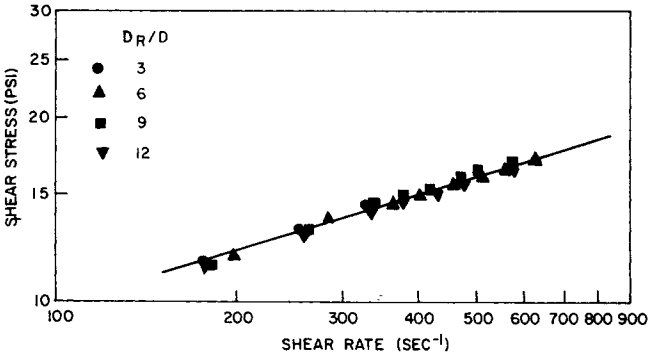

Fig. 3. Flow curves for high density polyethylene at 180°C.

$$\frac{\Delta P_{ent}}{\rho V^2/2g_c} = K_0 + K'/N_{Re} \qquad (2)$$

for non-Newtonian fluids, for which the power law

$$\tau_w = K \dot{\gamma}^n \qquad (3)$$

holds. It is to be noted in Equation (2) that the dimensionless coefficients K_0 and K' are functions of n as well as β, and that N_{Re} may be calculated by (*13*)

$$N_{Re} = \frac{\rho D^n V^{2-n}}{K_p 8^{n-1}\left(\frac{3n+1}{4n}\right)^n} \qquad (4)$$

It can be seen from Equations (2) through (4) that for Newtonian fluids ($n = 1$) coefficients K_0 and K' depend on β only.

In order to prepare plots of the dimensionless entrance pressure drop versus Reynolds number, one needs first to construct flow curves (plots of shear stress versus shear rate) to see if the material studied may be described by the power law. Construction of flow curves can readily be made in our case by use of the axial pressure profiles shown in Figure 1. That is because the true shear stress τ_w can be calculated by

$$\tau_w = \left(\frac{-\partial p}{\partial x}\right)\frac{D}{4} \qquad (5)$$

Note that the pressure gradient $(-\partial p/\partial x)$ can be obtained from the slope of the straight line portion of the axial pressure profile (see Figure 1). Note further that the true shear rate can readily be calculated from the experimentally measured volumetric flow rate and by use of the well-known Rabinowitch-Mooney equation.

Figure 3 shows flow curves for the material studied for D_R/D ratios of 3, 6, 9, and 12. As may be expected, the flow curves obtained yield single lines, which are independent of D_R/D ratio (that is, independent of the variation in the reservoir diameter). This indicates that an L/D ratio of 20 chosen for the study is long enough to ensure fully developed flow for the material used, and is in agreement with the earlier results based on the measurements of die swell and exit pressure (*1*). It is seen from Figure 3 that the material follows the power law over the range of shear rate studied. Calculated values of K and n in Equation (3) are 2.74 and 0.2815, respectively.

Having obtained numerical values of K and n in the power law, one can now calculate Reynolds number by use of Equation (4), and then prepare plots of the dimensionless entrance pressure drops versus Reynolds number, which are shown in Figure 4. It is seen, as may be expected, that the dependence on D_R/D ratio (and hence on β) is clearly shown, and that the plots are correlated by the expression

$$\frac{\Delta P_{ent}}{\rho V^2/2g_c} = K'/N_{Re} \qquad (6)$$

over the range of Reynolds number studied. Note that Equation (6) is a special case of Equation (2) with the coefficient $K_0 = 0$, and K' is a function of β alone in this case because n has a fixed value.

Sylvester and Rosen (*12*) have recently reported that dilute polymer solutions employed in their study follow the correlation given by Equation (2). Both Astarita and Greco (*14*) and Sylvester and Rosen (*12*) used Newtonian liquids and the former also presented their correlation given by Equation (2). The main difference between the present work and the previous (*12, 14*) is in the range of Reynolds number tested; that is, the present work which dealt with polymer melts has exceedingly low Reynolds numbers ($1.7 \times 10^{-4} \sim 1.5 \times 10^{-3}$), while the earlier work (*12, 14*) which dealt with solutions has much higher Reynolds numbers ($6 \sim 2{,}000$). Considering the magnitude of melt viscosities in general, the Reynolds number of polymer melts would be very small in almost all practical cases and hence Equation (6) appears to be a most useful correlation for them.

A few things are worth noting regarding the correlation observed here. First, the existence of the correlation by

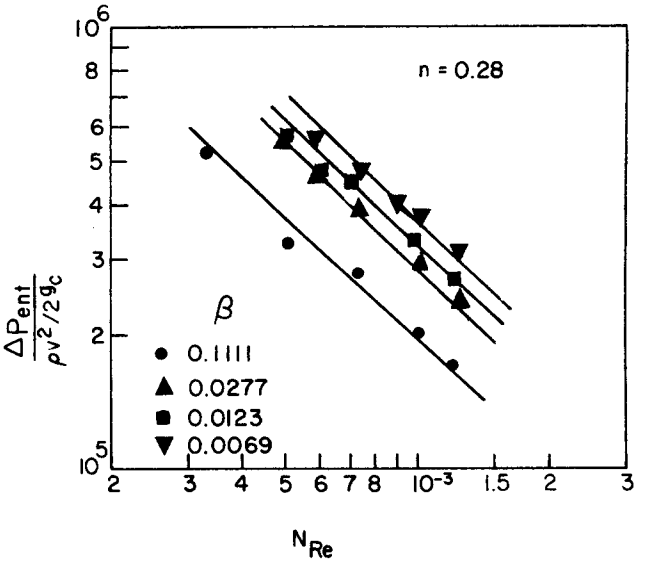

Fig. 4. Dimensionless entrance pressure drop versus Reynolds number for high density polyethylene at 180°C. with β as a parameter.

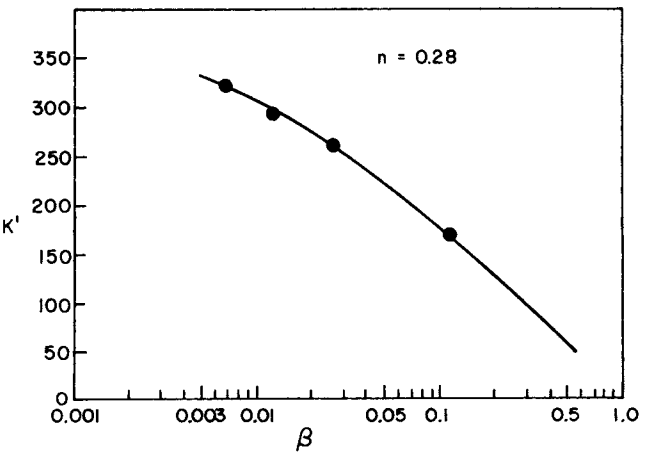

Fig. 5. Dimensionless coefficient K versus area contraction ratio for high density polyethylene at 180°C.

Equation (6) is in agreement with the creeping flow analysis by Weissberg (9). This is quite understandable in view of the very low Reynolds numbers encountered.

The main contribution to the very low Reynolds numbers for polymer melts comes from exceedingly high values of melt viscosity. This then suggests that any attempt to solve the equations of motion in the entrance region should be made by means of creeping flow analysis, instead by the boundary-layer analysis. It is to be noted that the creeping flow analysis by Weissberg (9) assumes that $\beta = 0$, that is, large D_R/D ratio. However, the present study indicates that the correlation given by Equation (6) holds at least for $0.00694 \leq \beta \leq 0.111$.

It is interesting, now, to see how coefficient K' in Equation (6) varies with the area contraction ratio β. Note that K' should approach 0 as β approaches 1, and that K' should approach a constant value as β approaches 0 (that is, infinite contraction). Figure 5 shows plots of K' versus β for the polymer melts studied. To the author's knowledge no such correlation has ever been published in the literature. At this point, it is worth noting that Sylvester and Rosen (*12*) concluded that coefficients K_0 and K' in Equation (2) should increase with β for $0 < \beta < 0.1616$ and that there must be maxima in K_0 and K' for $0 < \beta < 1$ because the coefficients K_0 and K' should vanish as β approaches 1. However, the conclusion made by Sylvester and Rosen (*12*) is based on limited experimental work which have only a single value of β for each fluid studied. Besides, it seems most unlikely (from a physical point of view), although not impossible, that K_0 and K' have maxima. Nevertheless, the correlation shown in Figure 5 clearly indicates that the speculation made by Sylvester and Rosen (*12*) is not justified.

A plot of friction factor versus Reynolds number can also be prepared by calculating the friction factor f with

$$f = \left(-\frac{\partial p}{\partial x}\right)\frac{D}{4}\Big/\frac{\rho v^2}{2g_c} \qquad (7)$$

Figure 6 gives such plots for the polymer melts studied, showing that the results are in good agreement with $f = 16/N_{Re}$. It is interesting to note that very recently Sylvester and Rosen (*12*) and Boger and Ramamurthy (*15*) obtained similar results with dilute polymer solutions and Newtonian liquids as well. Furthermore, Figure 6 shows a correlation which is independent of β. This is as expected because both dimensionless quantities f and N_{Re} contain variables which are pertinent only to the fully developed flow region of the tube. This fact, together with the correlation shown in Figure 6, supports the use of the experimental technique employed in the present study.

In order to investigate further the dependence of K' on n, measurements were taken at a fixed value of β of the entrance pressure drops for high density polyethylene at 200°, 220°, and 240°C., for polypropylene at 200°, 220°, and 240°C., for low density polyethylene at 200°C., and for polystyrene at 200° and 240°C. It is to be noted that variation of temperature changes the rheological properties of a polymer melt, and therefore variation of K' can be expected to occur. Figure 7 shows plots of $\Delta P_{ent}/\frac{\rho v^2}{2g_c}$ versus N_{Re} for several polymer melts at a fixed value of β, 0.0277. It is seen that the melts studied follow the correlation by Equation (6), and that K' decreases as n is increased, as is shown in Table 1. Note from Table 1 that the same value of n for two different materials can give rise to quite different values of K', and therefore one should examine the variation of K' with n for the same material. This point has

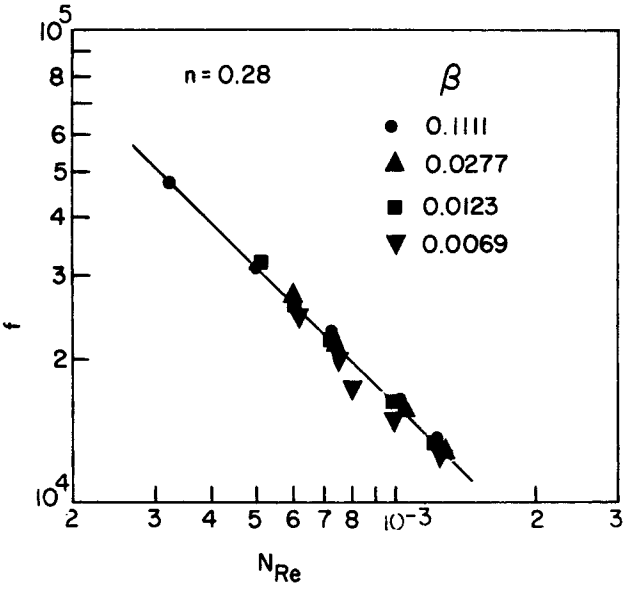

Fig. 6. Friction factor versus Reynolds number for high density polyethylene at 180°C. with different values of β.

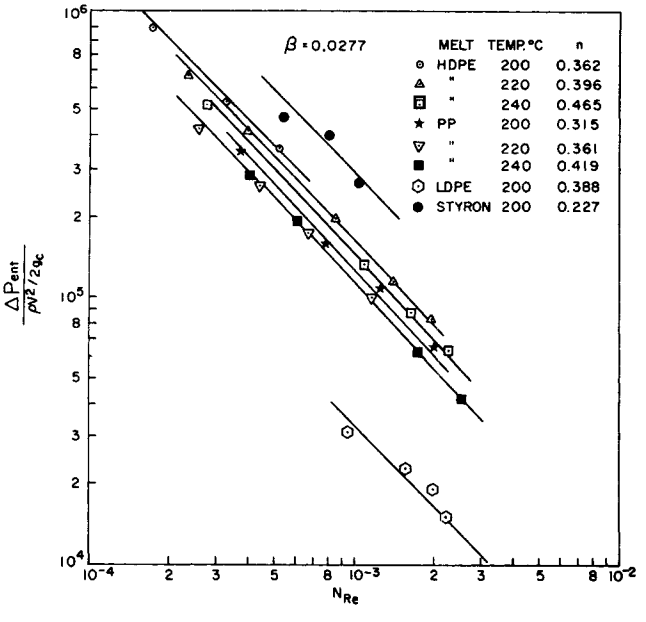

Fig. 7. Dimensionless entrance pressure drop versus Reynolds number for several polymer melts.

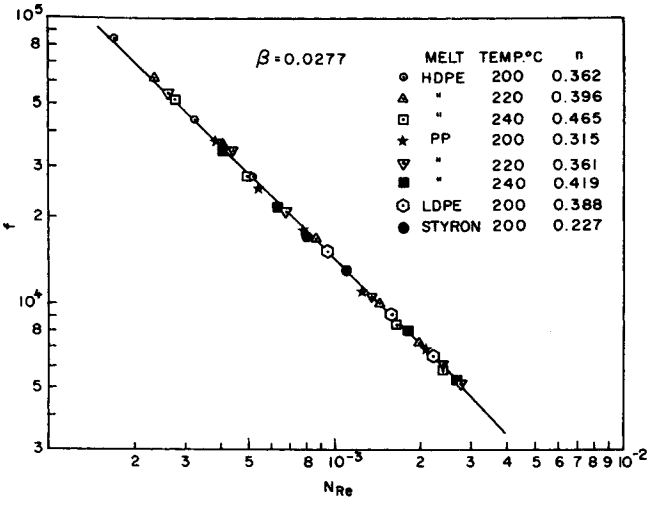

Fig. 8. Friction factor versus Reynolds number for several polymer melts.

TABLE 1. FLOW PROPERTIES OF POLYMER MELTS INVESTIGATED

Polymer	Sample code	Temperature, °C.	K, lb.$_f$/(sq. in.)(sec.$^{-n}$)	n, dimensionless	K', dimensionless
High density polyethylene	HDPE	200	2.280	0.362	167.0
		220	1.294	0.396	164.1
		240	0.739	0.465	141.3
Polypropylene	PP	200	1.739	0.315	132.6
		220	1.142	0.361	122.3
		240	0.687	0.419	115.1
Low density polyethylene	LDPE	200	1.166	0.388	31.1
Polystyrene	STYRON	200	2.955	0.227	235.7
		240	0.901	0.352	153.6

already been emphasized in connection with the variation of K' with β. Furthermore, plots of friction factor versus N_{Re} are shown in Figure 8, from which it is seen that all polymer melt samples yield a single line regardless of the rheological properties of the melts, showing good agreement with the theoretically predicted expression, $f = 16/N_{Re}$.

For viscoelastic fluids the total entrance pressure drop ΔP_{ent} may be divided into two parts: the viscous entrance pressure drop ΔP_{vis}, and the elastic entrance pressure drop ΔP_E (*16*). That is

$$\Delta P_{ent} = \Delta P_{vis} + \Delta P_E \tag{8}$$

Earlier Weissberg (9) presented an analysis for creeping Newtonian flow and gave the following expression

$$\Delta P_{vis} = \frac{12\eta Q}{D^3} \tag{9}$$

to estimate ΔP_{vis} for slow flow of Newtonian fluids. Since the flow of polymer melts is very slow ($N_{Re} = 2 \times 10^{-4} \sim 3 \times 10^{-3}$), we shall use Equation (9) to estimate ΔP_{vis} by replacing the Newtonian viscosity η with the shear-dependent viscosity corresponding to each value of the volumetric flow rate Q concerned.

Figure 9 shows plots of ΔP_E versus shear rate for several melt samples for $D_R/D = 6$, and Figure 10 for high density polyethylene for $D_R/D = 3$, 6, 9, and 12. These plots were prepared by use of Equations (8) and (9) and the data of total entrance pressure drops. It is seen from Figures 9 and 10 that a power law relation

$$\Delta P_E = a\,\dot{\gamma}^{\,b} \tag{10}$$

holds. It has been shown in the literature (*17*) that elastic properties (for example, die swell ratio and the exit pressure) may be plotted against shear stress, thereby eliminating the temperature dependence of the elastic properties. In view of this, plots of ΔP_E versus shear stress would yield a correlation which is independent of temperature, if the estimation of ΔP_E by means of Equations (8) and (9) were reasonably correct. Figure 11 shows plots of ΔP_E versus shear stress, indicating indeed the usefulness of Equation (9) for estimating the viscous entrance pressure drop. Our results indicate that about 90% of the total entrance pressure drops are due to the elastic loss, as shown in Table 2.

According to LaNieve and Bogue (*4*), the elastic loss is further made up of two parts: the dissipative loss due to any unusual flow patterns caused by the elasticity, and the elastic internal energy acquired by the fluid which is retained in the fluid and is then recoverable at the tube exit.

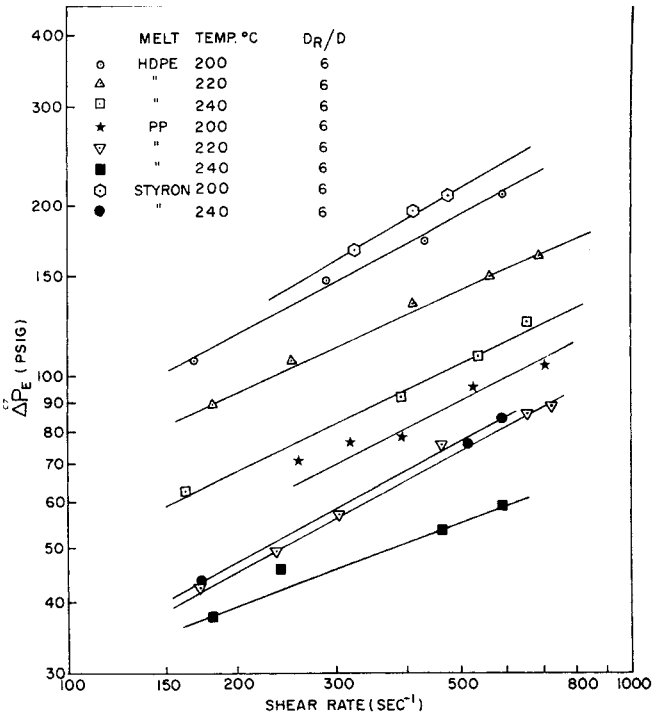

Fig. 9. Elastic entrance pressure drop versus shear rate for several polymer melts.

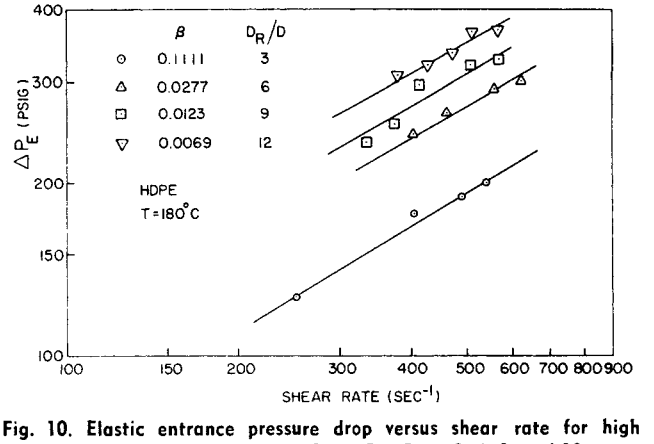

Fig. 10. Elastic entrance pressure drop versus shear rate for high density polyethylene at 180°C. for $D_R/D = 3$, 6, 9, and 12.

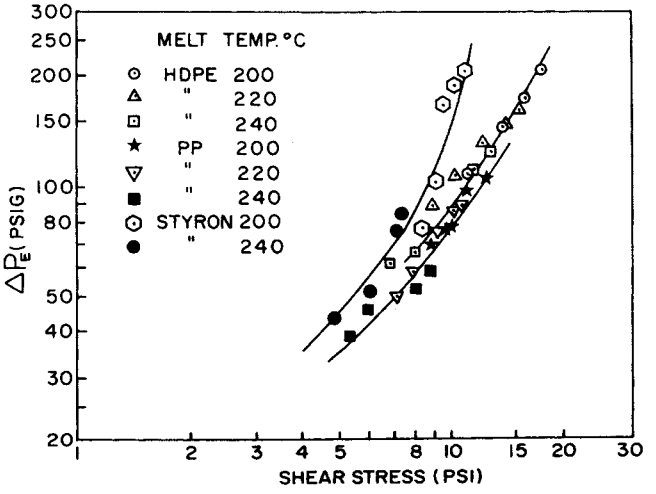

Fig. 11. Elastic entrance pressure drop versus shear stress for several polymer melts for $D_R/D = 6$.

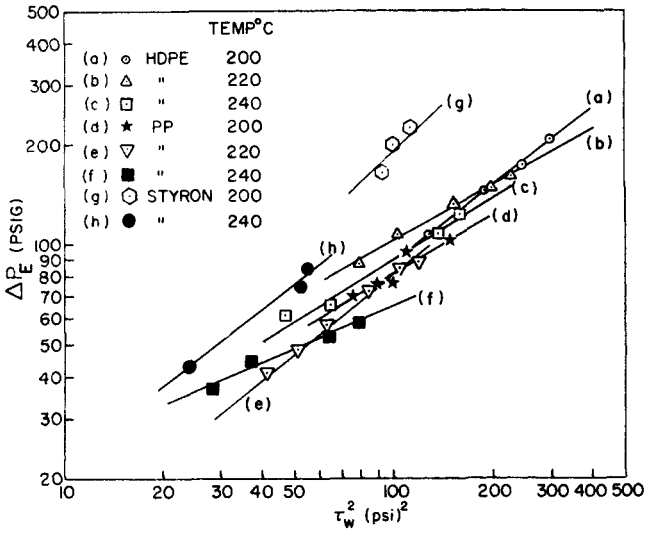

Fig. 12. Plots of ΔP_E versus τ_w^2 for several polymer melts.

TABLE 2. ELASTIC ENTRANCE PRESSURE DROPS OF POLYMER MELTS INVESTIGATED

Polymer	$\Delta P_E/\Delta P_{ent}$	$P_{exit}/\Delta P_E$
High density polyethylene	0.901	0.104
Polypropylene	0.868	0.153
Polystyrene	0.921	0.127

It would be interesting to estimate what fraction of the elastic loss is recoverable. Han (*10, 11*) has recently contended that the exit pressure is exactly the measure of recoverable elastic energy retained in the fluid. It should be noted that the exit pressure can be determined from the measurement of the axial pressure profiles (see Figure 1).

The last column in Table 2 gives the ratio of the exit pressure to the elastic entrance pressure drop for high density polyethylene, polypropylene, and polystyrene melts. The values given in Table 2 are the averages taken over the range of shear rate studied (200 to 850 sec.$^{-1}$) and at three temperatures: 200°, 220°, and 240°C. Deviation about the average value is about ± 10%. It is worth noting that a polymer melt which yields a higher value of $P_{exit}/\Delta P_E$ may be said to be more elastic than the sample yielding a lower value of $P_{exit}/\Delta P_E$. In view of this, polypropylene melt is the most elastic of the three polymers.

Last, it is to be noted that recently Sylvester and Rosen (*12*) suggested a method, based on the assumption of Hooke's law in shear, of estimating the elastic entrance pressure drop. This can be tested by plotting ΔP_E versus τ_w^2, as shown in Figure 12. It is seen from Figure 12 that the materials used do not obey Hooke's law in shear over the range of shear rate encountered, giving rise to a slope less than 1.

CONCLUDING REMARKS

The present study clearly shows how the reservoir-to-capillary diameter ratio influences the entrance pressure drops in polymer melts. This information is very useful for the design of various devices for processing molten polymers. The correlation between the dimensionless entrance pressure drop and Reynolds number obtained in the present study suggests the use of creeping flow analysis to carry out future theoretical studies concerning the entrance region flow of polymer melts. Finally, the correlation shown in Figure 5 is believed to clarify some confusions apparent in the literature.

It may be worth noting that the present study refers to a flat die entrance (180 deg. included angle) only. A study also has been made by the author of the effect of die entry angle on the entrance pressure drops and will be reported in a future publication.

NOTATION

a, b = constants in Equation (10)
c, d = constants in Equation (1)
D = tube diameter, in.
D_R = reservoir diameter, in.
f = friction factor, dimensionless
g_c = conversion factor, (32 lb.$_m$) (ft.)/(lb.$_f$) (sec.^{2})
L = capillary length, in.
K_0, K' = dimensionless coefficient as defined in Equation (2)
K = fluid consistency as defined in Equation (3), lb.$_f$/(sq.in.)(sec.$^{-n}$)
K_p = fluid consistency defined by g_cK, lb.$_m$/(in.)(sec.$^{2-n}$)
n = flow index as defined in Equation (3), dimensionless
N_{Re} = Reynolds number, dimensionless
ΔP_{ent} = entrance pressure drop, lb.$_f$/sq.in.
ΔP_E = elastic entrance pressure drop, lb.$_f$/sq.in.
ΔP_{vis} = viscous entrance pressure drop, lb.$_f$/sq.in.
Q = volumetric flow rate, cu.in./sec.
$\frac{-\partial p}{\partial x}$ = axial pressure gradient, lb.$_f$/cu.in.
V = average velocity, in./sec.

Greek Letters

β = area contraction ratio ($= D^2/D_R^2$)
$\dot{\gamma}$ = true shear rate, sec.$^{-1}$
ρ = fluid density, lb.$_m$/cu.in.
τ_w = true wall shear stress, lb.$_f$/sq.in.
η = viscosity, (lb.$_f$)(sec.)/sq.in.

LITERATURE CITED

1. Han, C. D., and M. Charles, *AIChE J.*, **16**, 499 (1970).
2. Bagley, E. B., *J. Appl. Phys.*, **28**, 624 (1957).
3. Philippoff, W., and F. H. Gaskins, *Trans. Soc. Rheol.*, **2**, 263 (1958).
4. LaNieve, H. L., and D. C. Bogue, *J. Appl. Polymer Sci.*, **12**, 353 (1968).
5. Bogue, D. C., *Ind. Eng. Chem.*, **51**, 874 (1959).
6. Collins, M., and W. R. Schowalter, *AIChE J.*, **9**, 804 (1963).
7. Denn, M. M., *Chem. Eng. Sci.*, **22**, 395 (1967).
8. Metzner, A. B., and J. L. White, *AIChE J.*, **11**, 989 (1965).
9. Weissberg, H. L., *Phys. Fluids*, **5**, 1033 (1962).
10. Han, C. D., M. Charles, and W. Philippoff, *Trans. Soc. Rheol.*, **13**, 455 (1969).
11. *Ibid.*, **14**, 393 (1970).
12. Sylvester, N. D., and S. L. Rosen, *AIChE J.*, **16**, 967 (1970).
13. Metzner, A. B., and J. C. Reed, *ibid.*, **1**, 434 (1955).
14. Astarita, G., and G. Greco, *Ind. Eng. Chem. Fundamentals*, **7**, 27 (1968).
15. Boger, D. V., and A. V. Ramamurthy, *AIChE J.*, **16**, 1088, (1970).
16. Boles, R. L., H. L. Davis, and D. C. Bogue, *Polymer Eng. Sci.*, **10**, 24 (1970).
17. Han, C. D., *AIChE J.*, **16**, 1087 (1970).

Manuscript received February 18, 1971; revision received April 7, 1971; paper accepted April 8, 1971.